

PRESSURE DEPENDENCE OF RAMAN-ACTIVE MODE FREQUENCIES IN SULVANITE  
 $\text{Cu}_3\text{NbS}_4$  TERNARY COMPOUND

Menjamin Salas<sup>1,4</sup>, Pedro Grima-Gallardo<sup>1</sup>, Chrystian Power<sup>1</sup>, Miguel Quintero<sup>1</sup>, Miguel Soto<sup>1</sup>,  
 José M. Briceño<sup>2</sup>, Hector Romero<sup>3</sup>

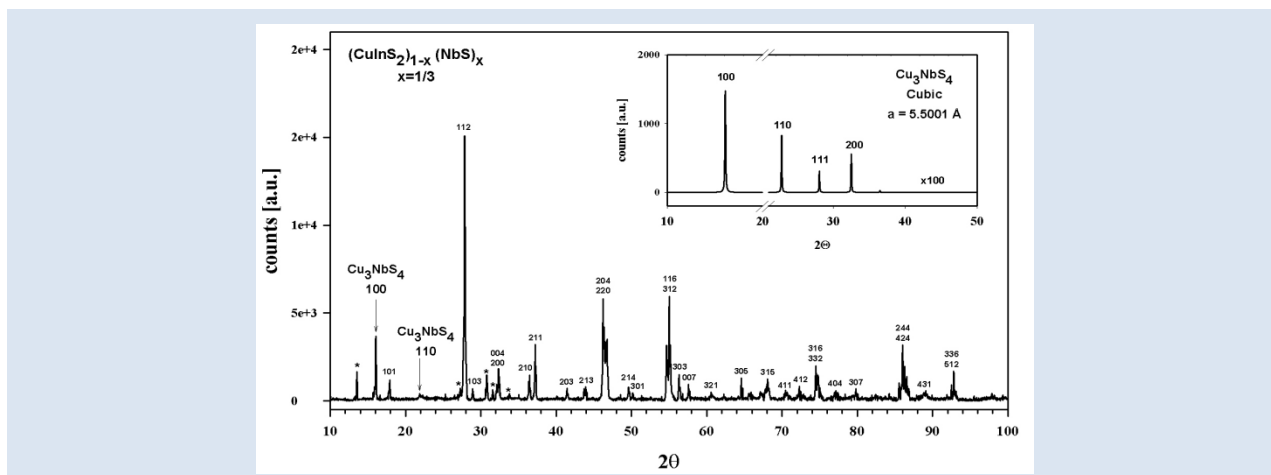
1: Centro de Estudios en Semiconductores (C.E.S.). Departamento de Física, Facultad de Ciencias, Universidad de Los Andes, Mérida 5101-Venezuela.

2: Laboratorio de Análisis Químico y Estructural (LAQUEM), Departamento de Física, Facultad de Ciencias, Universidad de Los Andes, Mérida 5101-Venezuela.

3: Laboratorio de Magnetismo, Departamento de Física, Facultad de Ciencias, Universidad de Los Andes (ULA), Mérida 5101, Venezuela.

4: Programa Ciencias de la Educación, Vicerrectorado de Producción Agrícola (VPA), Universidad Nacional Experimental de Los Llanos Occidentales "Ezequiel Zamora" (UNELLEZ), vía Biscucuy, Mesa de Cavacas, Guanare, Estado Portuguesa, Venezuela.

\* e-mail: albertm@ula.ve



## ABSTRACT

Pressure dependence of Raman-active mode frequencies and linewidths in  $\text{Cu}_3\text{NbS}_4$  ternary compound has been investigated up to 30 Kb (at room temperature) using focalized micro-Raman technique in a diamond anvil high pressure cell. Seven Raman-active modes frequencies were clearly observed in the pressure range studied and the variation of their respective Raman shift frequency as a function of pressure were given. A structural phase transition at  $25 \pm 5$  Kb previously reported in literature was confirmed.

Keywords:  $\text{Cu}_3\text{NbS}_4$ , alloys, x-ray diffraction, scanning electron microscopy, raman scattering.

## DEPENDENCIA CON LA PRESIÓN DE LAS FRECUENCIAS DE LOS MODOS RAMAN ACTIVOS DEL COMPUESTO TERNARIO DE $\text{Cu}_3\text{NbS}_4$ .

## RESUMEN

Se investigó la dependencia con la presión (hasta 30 Kb y a temperatura ambiente) de las frecuencias y los anchos de línea de los modos Raman activos del compuesto ternario  $\text{Cu}_3\text{NbS}_4$  usando una celda de presión de diamante y la técnica de micro-Raman focalizado. Se observaron claramente siete modos de frecuencia Raman-activos en el rango de presión estudiado y se reportan sus variaciones en función. Se confirmó una transición de fase estructural a  $25 \pm 5$  Kb anteriormente reportada en literatura.

Palabras Claves:  $\text{Cu}_3\text{NbS}_4$ , aleaciones, difracción de rayos x, microscopio electrónica de barrido, dispersión raman.

## 1. INTRODUCTION

Ternary compounds belonging to the family  $\text{Cu}_3\text{MSe}_4$  ( $\text{M} = \text{V}, \text{Nb}, \text{Ta}$ ) are interesting materials due principally to their potential applications as electronic devices, especially as light modulators [1–6]. Several authors have reported the preparation of this type of materials [1, 7–9] and have associated their structures with that of the mineral sulvanite ( $\text{Cu}_3\text{VS}_4$ ), which crystallizes in the cubic symmetry, space group  $P\bar{4}3m$  ( $N^\circ$  215) [10] with one molecule unit (eight atoms) per unit cell. In Table I we summarize the known structural parameters and the bandgap energies of sulvanita-type compounds at ambient conditions.

**Table I.** Lattice parameters and optical energy gaps of Cu-M-VI<sub>4</sub> compounds (M: S, Se, Te and VI: S, Se, Te) reported in literature.

Compound	$a$ [Å]	$E_g$ [eV]
$\text{Cu}_3\text{VS}_4$	5.3912 [11]	1.3 [12]
$\text{Cu}_3\text{VSe}_4$	5.5636 [13]	---
$\text{Cu}_3\text{VTe}_4$	---	---
$\text{Cu}_3\text{NbS}_4$	5.5001 [14]	---
$\text{Cu}_3\text{NbSe}_4$	5.638 [15]	---
$\text{Cu}_3\text{NbTe}_4$	5.9217 [23]	---
$\text{Cu}_3\text{TaS}_4$	5.5185 [16]	2.70 [17]
$\text{Cu}_3\text{TaSe}_4$	5.6625 [16] 5.6600 [9]	2.35 [17]
$\text{Cu}_3\text{TaTe}_4$	5.9283 [16] 5.930 [18]	---

The mechanical representation with eight atoms per cell decomposes as  $\Gamma_{\text{mec}} = A_1 \otimes E \otimes 2F_1 \otimes 5F_2$  where the  $A_1$  and  $E$  modes are only Raman active, four  $F_2$  modes are both Raman and infrared active, and the acoustic  $F_2$  modes and the two  $F_1$  mode are inactive. The lattice vibrations of  $\text{Cu}_3\text{NbS}_4$  under high pressure have been investigated by Petritis *et al* [19] but they observed a very weak Raman signal and a high level of the background noise that prohibits the detection of any reliable peak for the weakest modes as a function of pressure. However, a phase transition at about 25 Kb was reported characterized by a rapid decrease of the Raman activity. They also reports no remarkable changes of the FWHM within the experimental accuracy and the observation of a satellite peak with an  $A$  symmetry not predicted by the group-theoretical analysis. In this work, using

micro-Raman technique the seven Raman-active modes were clearly observed and followed as a function of the applied pressure until the transition at around 25 Kb. The FWHM of the  $A_1$  structure and their satellite  $A_1'$  were also obtained as a function of pressure.

## 2. EXPERIMENTAL PART

The  $\text{Cu}_3\text{NbS}_4$  phase was obtained as a secondary phase embeded in a  $\text{CuInS}_2$  matrix, when the alloy  $(\text{CuInS}_2)_{1-x}(\text{NbS})_x$  with  $x=1/3$  was prepared by the usual melt and anneal technique. The product was characterized by X-ray powder diffraction (XRD) and Scanning Electron Microscopy (SEM). Experimental details of these techniques can be found elsewhere [20]. Raman spectra were recorded in the back-scattering geometry using a micro-Raman, triple grating system (DILOR XY800) equipped with a cryogenic CCD detector. The spectral resolution of the system was about  $1 \text{ cm}^{-1}$ . For excitation, the 514.5 nm line of an argon laser was focused on the sample by means of a 100X objective, while the laser power was kept below 2 mW, in order to avoid laser-heating effects on the probed material and the concomitant softening of the observed Raman peaks. For pressure-dependent measurements a gasketed diamond anvil high pressure cell was used. A small sample is introduced in a hole of about 80  $\mu\text{m}$  height and 200  $\mu\text{m}$  in diameter opened in the gasket. Some small rubies crystals were also introduced as a pressure gauge together with a drop of 4:1 methanol-ethanol mixture as pressure transmitting medium. The phonon frequencies were obtained by fitting Lorentzian functions to the experimental peaks.

## 3. RESULTS AND DISCUSSION

### 3.1 X-Ray Diffraction (XRD)

The XRD pattern of the alloy  $(\text{CuInS}_2)_{1-x}(\text{NbS})_x$  ( $x=1/3$ ) is displayed in Figure 1. In this pattern, the characteristic peaks of the  $\text{CuInS}_2$  chalcopyrite structure are dominant together with the stronger peak of the  $\text{Cu}_3\text{NbS}_4$  corresponding to the  $hkl=100$  Miller indices at  $2\Theta=16.102$ . In the insert, the calculated diffraction pattern of  $\text{Cu}_3\text{NbS}_4$  using conventional software is also showed (after the break the intensity is  $\times 100$ ). Some other unidentified peaks in the diffraction pattern are labeled with asterisks.

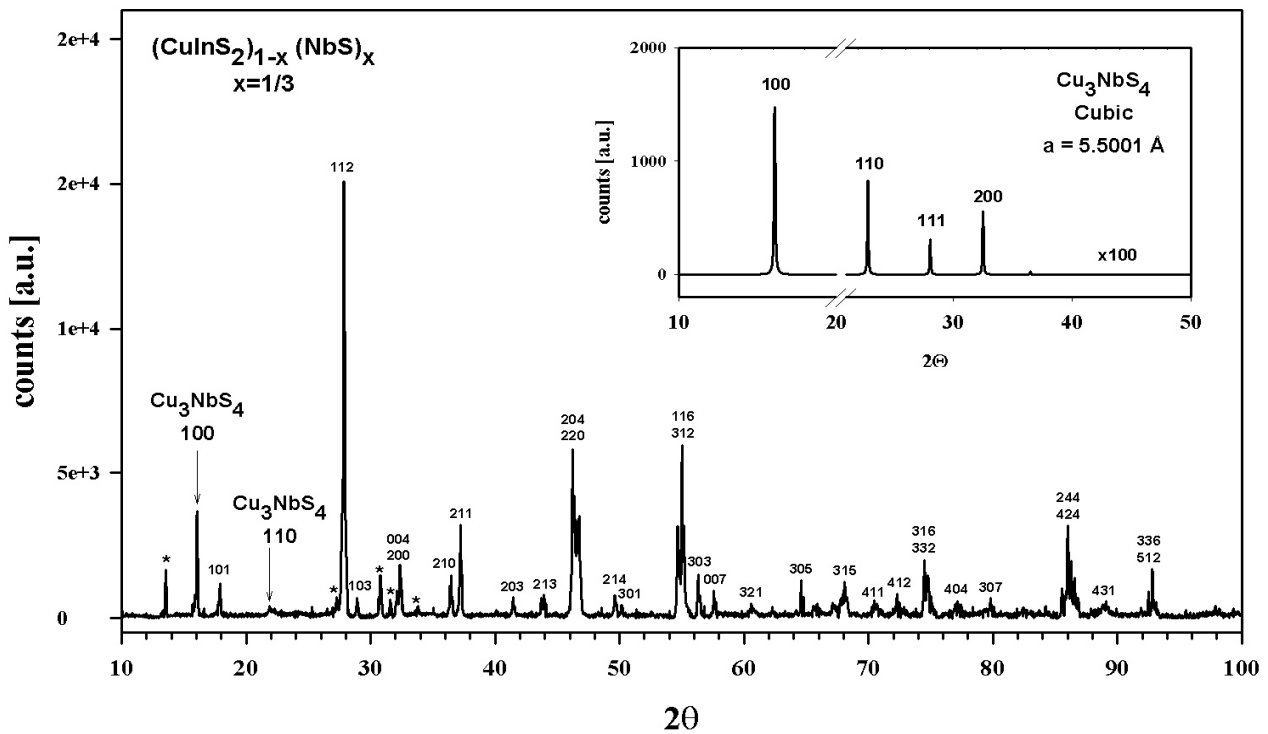


**Figure 1.** Experimental XRD diffraction pattern of the alloy  $(\text{CuInS}_2)_{1-x}(\text{NbS})_x$  ( $x=1/3$ ). Except when they are expressly indicated, the Miller indices correspond to the  $\text{CuInS}_2$  phase. Some not identified peaks are labeled with asterisks. In the insert, the calculated diffraction pattern for  $\text{Cu}_3\text{NbS}_4$  with  $a=5.5001 \text{ \AA}$  (for  $2\theta > 20^\circ$  the intensity is multiplied by 100).

**Table II.** Stoichiometric analysis obtained by Scanning Electron Microscopy (SEM) technique

Element	Experimental atomic concentration (%)	Experimental atomic concentration (%)	Nominal atomic concentration (%)	Nominal atomic concentration (%)
	phase I	phase II	$\text{CuInS}_2$	$\text{Cu}_3\text{NbS}_4$
S	50±5	53±5	50	50
Cu	25±3	34±3	25	37.5
Nb	---	13±2	---	12.5
In	25±3	---	25	---

### 3.2 Scanning Electron Microscopy (SEM)

The stoichiometric analysis obtained using Scanning Electron Microscopy (SEM) technique, of each phase observed, is given in Table II. The phase I is  $\text{CuInS}_2$  whereas phase II is  $\text{Cu}_3\text{NbS}_4$ .

### 3.3 Raman Scattering

Raman scattering were obtained as a function of pressure in steps of approximately 1-2 Kb from ambient to 31Kb. No relevant changes in the structures were observed up to 24 Kb. In figure 2 the measured Raman shift frequencies at 1.25 Kb and in Figure 3 at 21.2, 24.2 and 30.0 Kb are shown. Seven

structures can clearly be seen and followed until the phase transition and their respective variation with pressure is given in Figure 4. In Table III, the values obtained by Petritis *et al* are compared with those obtained in this work.

Although the alloy  $(\text{CuInS}_2)_{1-x}(\text{NbS})_x$  ( $x=1/3$ ) is not single phase, the micro-Raman technique together with the diamond anvil cell permitted to focus the laser beam in a few microns inside the cell on the desired phase, as it can be seen in figure 2, where only the structures corresponding to  $\text{Cu}_3\text{NbS}_4$  are clearly observed. The results are in complete agreement with those obtained previously [19] for the modes  $A_1$ ,  $A_1'$  and E only that we have obtained

a best precision in  $d\omega/dp$  values and, in addition, the  $d\omega/dp$  values for the modes  $F_2^a$ ,  $F_2^b$ ,  $F_2^c$  and  $F_2^d$  are obtained for first time in our knowledge. The phase transition at  $25 \pm 5$  Kb previously reported in literature was confirmed. This transition is

characterized by a drastic reduction of the Raman signal and observation of two structures at 391.6 and 176.4  $\text{cm}^{-1}$ , no one of them belonging to  $\text{CuInS}_2$  which  $A_1$  structure has been observed at 290  $\text{cm}^{-1}$  at ambient conditions [21].

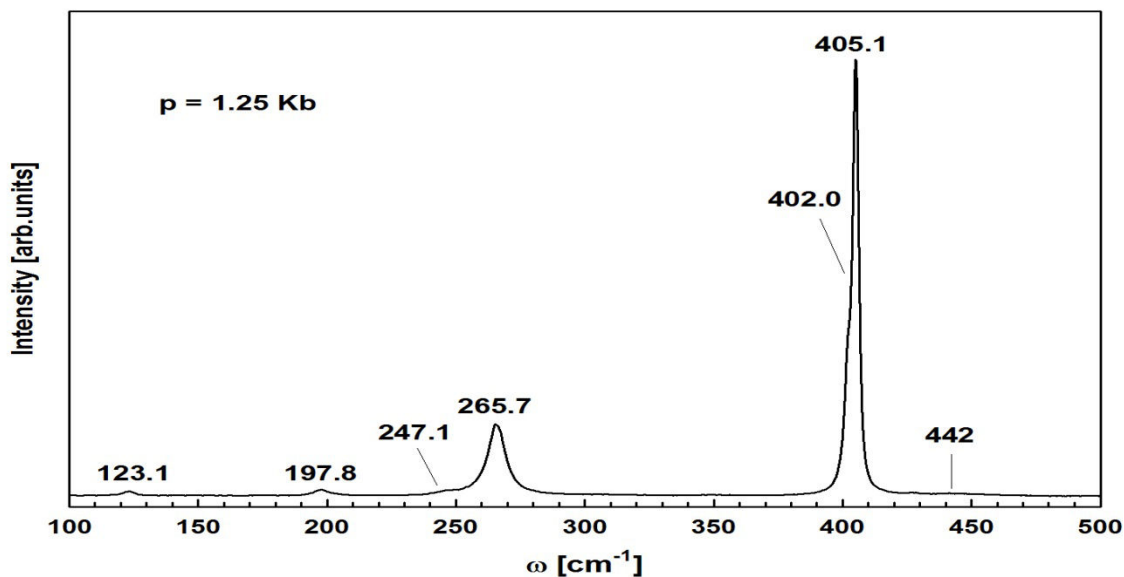


**Figure 2.** Raman scattering of the  $\text{Cu}_3\text{NbS}_4$  phase at 1.25 Kb. Values of the Raman shift frequencies and assignment modes are labeled on the top of each structure.

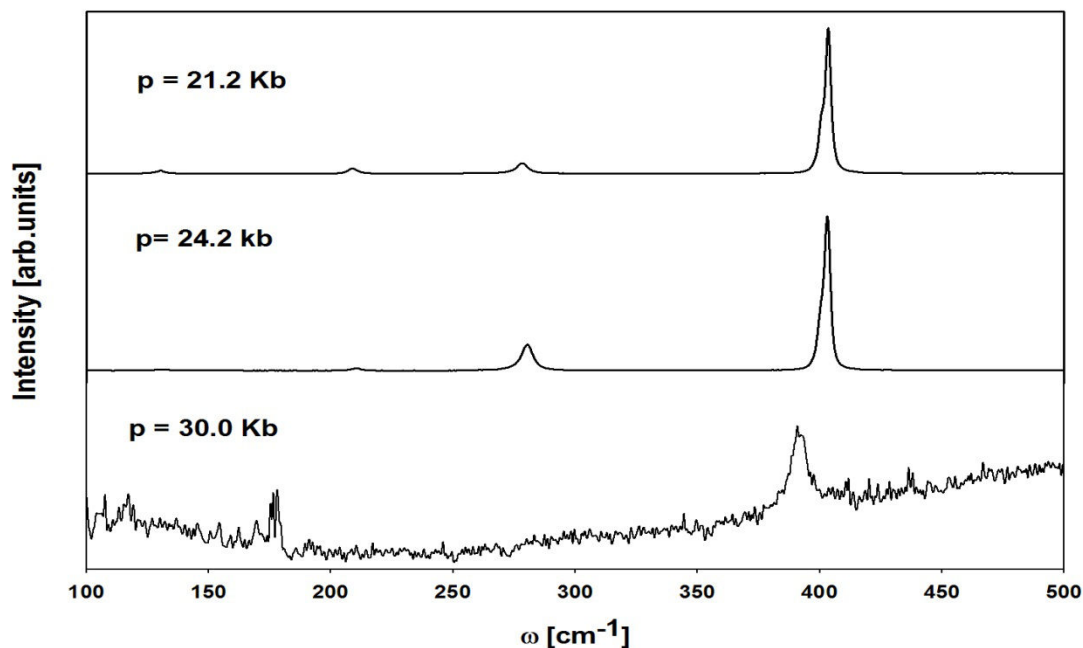


**Figure 3.** Raman scattering of the  $\text{Cu}_3\text{NbS}_4$  phase at 21.2, 24.2 and 30.0 Kb.

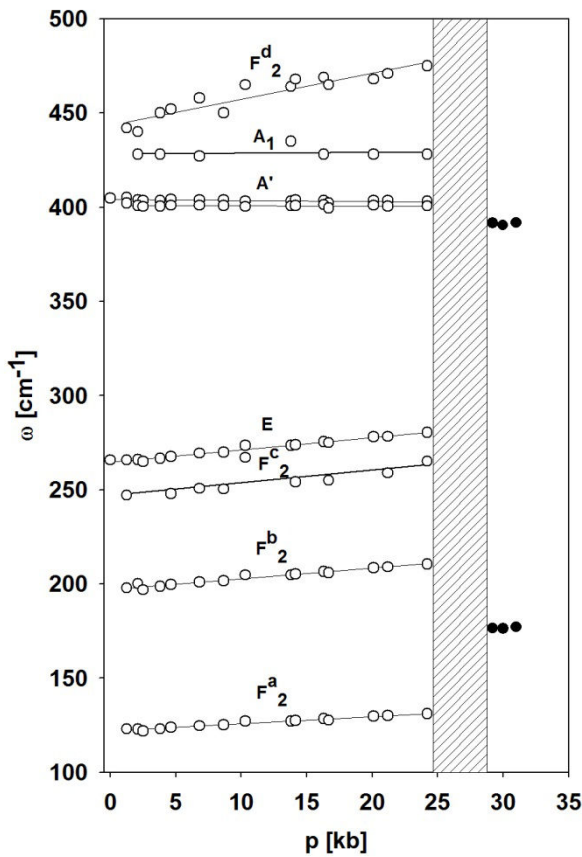


**Figure 4.** Variation of the Raman shift frequencies with applied pressure, from ambient to 35 Kb. Empty circles before phase transition and full circles after phase transition. The shaded area represents the region where a transition phase occurs.

An interesting feature of these compounds ( $\text{Cu}_3\text{NbS}_4$

**Table III.** Frequency ( $\text{cm}^{-1}$ ), assignment of vibrational modes and their dependence with pressure for the ternary compound  $\text{Cu}_3\text{NbS}_4$ .

Mode	Petritis et al [19] Infrared-reflectivity $P=0$		Petritis et al [19] Raman scattering as a function of pressure $\omega = \omega_0 + cP$	This work Raman Scattering as a function of pressure $\omega = \omega_0 + cP$	
	$\omega_0$	$\omega_0$	c	$\omega_0$	c (=d $\omega$ /dP)
$A_1$	404	403.7	$(0 \pm 3) \times 10^{-2}$	405.1	-0.05
$A_1'$	---	400.5	$(2 \pm 1) \times 10^{-2}$	402.0	-0.02
E	265.2	265.6	0.6	265.7	0.65
$F_2^a$	122.1	---	---	123.1	0.38
$F_2^b$	196.4	---	---	197.8	0.56
$F_2^c$	245.5	---	---	247.1	0.66
$F_2^d$	440.0	---	---	442	1.39

and  $\text{Cu}_3\text{TaS}_4$ ) is the presence of a satellite labeled  $A_1'$  which remains an open question up to now. Petritis *et al* discussed in detail the origin of this structure [19]: a) a double-phonon structure; b) a Jahn-Teller effect; c) a symmetry-lowering effect; d) an isotope effect; and e) an inversion of a small number of copper and niobium (or tantalum) atoms; no one of them gives a plausible explanation. In order to contribute at the discussion of this point, we have initiated a systematic study of the Raman shift spectra of others  $\text{Cu}_3\text{-M-VI}_3$  compounds (M: V, Nb, Ta; VI: S, Se, Te) and observed in preliminary results that this satellite is also observed in  $\text{Cu}_3\text{NbSe}_4$  [22]. This observation, that must be corroborated in the experiments on others compounds of this family, suggests that the presence of the satellite  $A_1'$  is inherent to the “eigenmotion” of the anion (S, Se or Te) in the sulvanite structure more than to an specific compound. In Figure 5 the FWHM of the  $A_1$  and  $A_1'$  structures are given as a function of pressure in the range from ambient to 24 Kb (in the edge of the phase transition). It can be clearly observed that the dependence of both structures with pressure is nearly the same, with a broad maximum at around 8 Kb, which confirms the twin-character of these two structures. A first sight analysis induces to justify this parabolic variation of the FWHM with pressure as a pre-transitional behavior: an initial disordering of the sulvanite phase followed by a reordering towards the new structure. Nevertheless, more experiments are in course in order to obtain a systematic analysis on these interesting compounds.

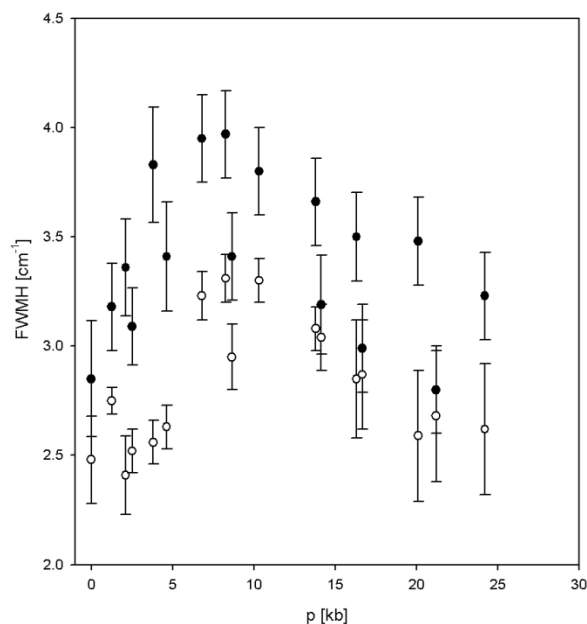


**Figure 5.** Variation of the FWHM of the  $A_1$  (full circles) and  $A_1'$  (empty circles) structures with the applied pressure.

#### 4. CONCLUSIONS

This paper is an experimental complement of [19] for the lattice vibrations of  $\text{Cu}_3\text{NbS}_4$ . All the optical active modes have been followed as a function of pressure until the phase transition at around 25 Kb and values of  $d\omega/dp$  were obtained with a better accuracy. The dependence with pressure of the FWHM of the  $A_1$  and  $A_1'$  structures are given.

#### 5. REFERENCES

- [1]. R. Nitsche, P. Wild, J. Appl. Phys. **38**, 5413 (1967).
- [2]. F. Zwick, H. Berger, M. Grioni, G. Margaritondo, L. Forro, J. La Veigne, D.B. Tanner, M. Onellion, Phys. Rev. **B59**, 7762, (1999).
- [3]. N. Shannon, R. Joynt, Solid State Commun. **115**, 411 (2000).
- [4]. M.L. Doublet, S. Remy, F. Lemoigno, J. Chem. Phys. **113**, 5879 (2000).
- [5]. S. Debus, B. Harbrecht, J. Alloys Compd. **338**, 253 (2002).
- [6]. Y. Aiura, H. Bando, R. Kitagawa, S. Maruyama, Y. Nishihara, K. Horiba, M. Oshima, O. Shiino, M. Nakatake, Phys. Rev. **B68**, 073408, (2003).
- [7]. A.E. Van Arkel, C. Crevecoeur, J. Less, Common Metals **5**, 177 (1963).
- [8]. E. Riedel, K. Ereku, S. Yüksel, Anorg. Allg. Chem. **465**, 131 (1980).
- [9]. G.E. Delgado, A.J. Mora, S. Durán, M. Muñoz and P. Grima-Gallardo, J. Alloys and Compounds **439**, 346–349 (2007).
- [10]. L. Pauling, R. Hultgren, Z. Kristallogr. **84**, 204 (1932).
- [11]. F.J. Trojer. The American Mineralogist, **51**, 890 (1966).
- [12]. D.M. Schleich and M. Rosso. Solid State Ionics, **5**, 383 (1981).
- [13]. K.O. Klepp and D. Gurtner. Zeitschrift für Kristallographie-New Crystal Structures, **215**, 4 (2000).
- [14]. M. Kars, A. Rebbah and H. Rebbah. Acta Cryst. **E61**, i180-i181, (2005).
- [15]. Y.J. Lu and J.A. Ibers. J. Solid State Chem., **107**, 58 (1993).
- [16]. K. Zitter and J. Schmand. Mat. Res. Bull. **19**, 801 (1984).
- [17]. P.F. Newhouse, P.A. Hersh, A. Zakutayev, A. Richard, H.A.S. Platt, D.A. Keszler, J. Tate, Thin Solid Films **517**, 2473–2476 (2009).
- [18]. J. Li, H.Y. Guo, D.M. Proserpio and A. Sironi, J. Solid State Chemistry, **117**, 247 (1995).
- [19]. D. Petritis, G. Martínez, C. Levy-Clement and O. Gorochoy, Phys. Rev. **B23**, 6773 (1981).
- [20]. P. Grima-Gallardo, M. Muñoz-Pinto, S. Durán-Piña, G.E. Delgado, M. Quintero, J.M. Briceño and J. Ruiz, Phys. Stat. Sol. (a) **204**, 1093 (2007).
- [21]. S-H. Wei and R. Scheer, Phys. Rev. **B71**, 054303 (2005).
- [22]. P. Grima-Gallardo, Ch. Power, M. Salas, M. Quintero, J.M. Briceño and H. Romero, to be published.
- [23]. G.E. Delgado, A.J. Mora, P. Grima-Gallardo, S. Durán, M. Muñoz, M. Quintero, Chalcogenide Letters **6**, 335 (2009).